

# Effect of Extrusion Temperatures on Microstructures and Mechanical Properties of Mg-6Zn-1Mn-4Sn-0.5Y Alloy

Hu Guangshan<sup>1,2</sup>, Zhang Dingfei<sup>1,2</sup>, Tang Tian<sup>1,2</sup>, Jiang Luyao<sup>1,2</sup>, Pan Fusheng<sup>1,2</sup>

<sup>1</sup>Chongqing University, Chongqing 400045, China; <sup>2</sup>National Engineering Research Center for Magnesium Alloys, Chongqing 400044, China

**Abstract:** The microstructural evolution and the mechanical properties of Mg-6Zn-1Mn-4Sn-0.5Y wrought alloy extruded at 360 and 420 °C were investigated by optical microscopy (OM), X-ray diffraction (XRD), scanning electron microscopy (SEM), electron back scattered diffraction (EBSD) and tensile test. The results show that the phase compositions of as-cast and extruded alloys consist of  $\alpha$ -Mg, Mn, Mg<sub>7</sub>Zn<sub>3</sub>, Mg<sub>2</sub>Sn, and MgSnY phases. As the extrusion temperature increases from 360 °C to 420 °C, dynamic recrystallization completes and grain growth occurs. The yield strength, the ultimate tensile strength and the elongation decrease from 259 MPa, 350 MPa and 18.3% to 239 MPa, 332 MPa and 12.5%, respectively. The theoretical calculations combined with the experimental results reveal that fine grain strengthening and solid solution strengthening play the dominating role in the enhancement of yield strength.

**Key words:** Mg-6Zn-1Mn-4Sn-0.5Y alloy; extrusion temperatures; phase compositions; mechanical property

In order to reduce weight and improve fuel consumption in automobiles and other transportation vehicles, magnesium (Mg) alloys become very attractive as structure materials for their high specific strength and low density<sup>[1-3]</sup>. However, their low strength and poor formability at room temperature restrict the applications. For expanding the applications scope of Mg alloys, the development of new high strength wrought Mg alloys have attracted great interest<sup>[4-6]</sup>.

Recent investigations have revealed that the strength of Mg alloys can be enhanced by means of thermal deformation, multi-stage aging and alloying<sup>[7]</sup>. Hot extrusion as one of thermal deformation methods, is widely used to process wrought Mg alloys for its technical and economical advantages<sup>[8]</sup>. During hot extrusion, dynamic recrystallization (DRX) occurs easily and the grains get refined<sup>[2,9]</sup>. The Hall-Petch coefficient of Mg alloys is reported to be 170~400 MPa  $\mu\text{m}^{1/2}$ , which is much higher than that of aluminum alloys (70 MPa  $\mu\text{m}^{1/2}$ )<sup>[10-12]</sup>. Therefore, strengthening via hot extrusion is an effective way for Mg alloys. Some investigations have shown that the grains of the as-extruded Mg alloys are

obviously refined by the occurrence of DRX. The average grain sizes of the extruded alloys increase with the increasing of extrusion temperature<sup>[4,13-15]</sup>.

In general, the extrusion temperatures play an important role in the microstructural evolution and strength enhancement of as-extruded Mg alloys. A newly developed Mg-6Zn-1Mn-4Sn-0.5Y (wt%) alloy exhibits a promising potential as structural materials for its high strength. However, the microstructural evolution and mechanical properties of the alloy extruded at different temperatures need further study. In the present study, the effects of extrusion temperatures on the microstructural evolution and mechanical properties of Mg-6Zn-1Mn-4Sn-0.5Y alloy were investigated.

## 1 Experiment

Mg-6Zn-1Mn-4Sn-0.5Y (ZMT614-0.5Y) alloy was prepared by high-purity Mg (>99.90%, mass fraction), Zn (>99.95%), Sn (>99.90%) and Mg-30.00%Y and Mg-5.10%Mn (all in wt%) master alloys which were melted in a ZG-0.01 vacuum induction melting furnace in Ar atmosphere. Then the melts

Received date: April 14, 2015

Foundation item: National Great Theoretic Research Project (2013CB632200); International Cooperation Project (2010DFR50010); Chongqing Science & Technology Support Project (CSTC2013jcyjC60001)

Corresponding author: Zhang Dingfei, Ph. D., Professor, National Engineering Research Center for Magnesium Alloys, Chongqing University, Chongqing 400044, P. R. China, Tel: 0086-23-65112491, E-mail: zhangdingfei@cqu.edu.cn

Copyright © 2016, Northwest Institute for Nonferrous Metal Research. Published by Elsevier BV. All rights reserved.

were cast into ingots with diameter of 80 mm. The as-cast ingots were homogenized at 420 °C for 12 h, and then extruded into bars with 16 mm in diameter at 360 and 420 °C with the extrusion ratio of 25. The chemical compositions of as-cast alloy were analyzed by XRF-1800 CCDE sequential X-ray fluorescence spectrometer. It was Mg-6.14Zn-0.91Mn-4.38Sn-0.50Y for ZMT614-0.5Y alloy.

Tensile tests were carried on a SANS CMT-5105 electronic testing machine at room temperature. Samples for tensile tests had a cross-sectional diameter of 5 mm and a gauge length of 50 mm. The strain rate of the samples was  $10^{-3} \text{ s}^{-1}$ . The yield strength, ultimate tensile strength and elongation to fracture were averaged over 3 samples. The optical microstructures (OM) were observed by LEXT 2000 laser metallographic microscope. The microstructural morphologies and compound compositions of the alloys were examined using ESCAN VEGA II scanning electron microscope (SEM) equipped with an oxford INCA Energy 350 energy dispersive X-ray spectrometer (EDS). Phase components were characterized by a Rigaku D/max 2500PC X-ray diffractometer (XRD) using Cu K $\alpha$ . Electron back scattered diffraction (EBSD) analysis was carried out by JEOL-7001F scanning electron microscopy equipped with TSL OIM Analysis 5 software.

## 2 Results and Discussion

### 2.1 Microstructures of the as-extruded alloy

Fig.1 shows the microstructures of ZMT614-0.5Y alloy extruded at 360 and 420 °C. It can be seen that the grains become coarsened obviously when the extrusion temperature increases. The average grain size increases from 3.2  $\mu\text{m}$  to 5.7  $\mu\text{m}$ . Different-sized second phase particles are distributed randomly on the cross sections, as shown in Fig.1a and 1b. Several extrusion streamlines are parallel to the extrusion direction (ED) (Fig.1c and 1d). As extrusion temperature increases, the particles get coarse. The amount and aspect ratio of streamlines decrease.

Fig.2 shows the XRD patterns of as-cast and extruded samples. After extrusion, the phase compositions of the samples are not changed. However, the diffraction peaks which are detected between 20° and 40° cannot match the characteristic peaks of Mg-Zn, Mg-Zn-Y and other phases. Zhao et al.<sup>[16]</sup> reported that a ternary phase MgSnY was formed in Mg-Sn-Y system. Gorny and co-workers<sup>[17]</sup> revealed that MgSnY phase was formed and no any Mg-Zn-Y phases were detected in Mg-Zn-Sn-Y alloys. The characteristic peaks of MgSnY phase matches the new diffraction peaks perfectly, so the new phase should be MgSnY phase. As a result, the ZMT614-0.5Y alloy consists of  $\alpha$ -Mg, Mn, Mg<sub>7</sub>Zn<sub>3</sub>, Mg<sub>2</sub>Sn, and MgSnY phases both in as-cast and extruded conditions.

Fig.3 shows the SEM micrographs and EDS analysis of as-extruded samples. The EDS analysis shows that only Zn

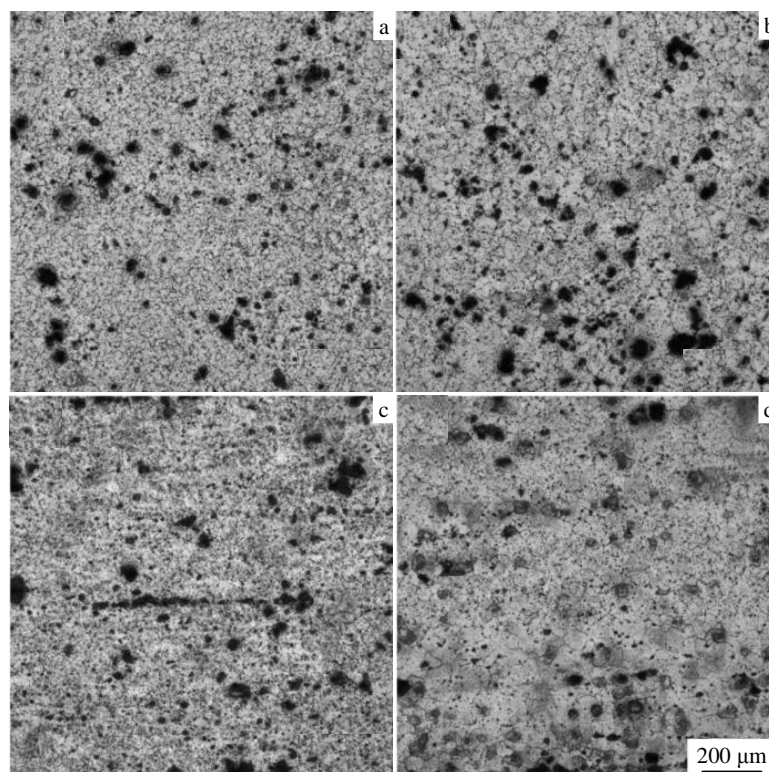


Fig.1 Optical micrographs of ZMT614-0.5Y alloy extruded at different temperatures: (a,c) 360 °C, (b,d) 420 °C; (a,b) perpendicular to the extrusion direction, (c,d) parallel to the extrusion direction

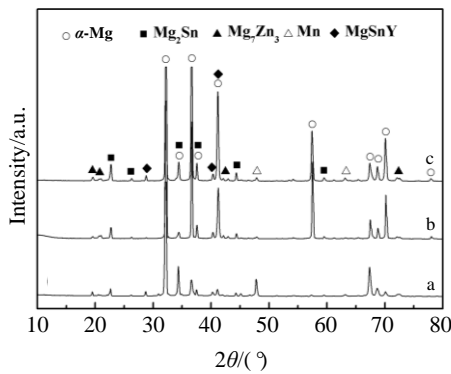


Fig.2 XRD patterns of ZMT614-0.5Y alloy in different states: (a-as-cast, b-extruded at 360 °C, and c-extruded at 420 °C)

and Sn elements dissolve into the matrix (point A and B). And the dissolved amount increases as the extrusion temperature increases. Extruded at 360 °C, several thick cuboid-shaped MgSnY and rod-shaped Mg<sub>2</sub>Sn phases are distributed in the matrix. The MgSnY and Mg<sub>2</sub>Sn particles get coarse and their amount decreases as the extrusion temperature increases. However, the number density of extremely fine particles decreases significantly when the extrusion temperature increases. Based on previous research and above analysis<sup>[2,13]</sup>, the fine particles should be Mg<sub>7</sub>Zn<sub>3</sub> phase.

For explaining the microstructural evolution precisely at different extrusion temperatures, the EBSD analysis was used. Fig.4 shows the inverse pole figures (IPFs) and pole figures (PFs) of the as-extruded samples on the cross sections. Different colors indicate different crystallographic orientations in

IPF maps (see digital version). DRX has been completed when extruded at 420 °C (Fig.4b). However, some unDRX regions are remained when extruded at 360 °C as shown in Fig.4a. The unDRX regions reveal blue color, indicating that the regions show (10 $\bar{1}$ 0)<sub>α</sub>. The average grain size of unDRX regions is 10.3 μm. IPFs show that the predominant texture in both alloys has the (11 $\bar{2}$ 0) normal close to the ED. This texture is commonly confirmed in as-extruded Mg alloys<sup>[18]</sup>. The texture is weak, whose maximum intensity is only 4.06. The basal and prismatic PFs show that the intensity of the texture exhibits a slight decrease as extrusion temperature increases, which means that the anisotropy of as-extruded alloys decreases when the extrusion temperature increases.

Fig.5 shows the corresponding misorientation angle and Schmid factors of the as-extruded samples on the cross sections. It is seen that the grain boundary misorientation distribution changes slightly with the extrusion temperature increases. The fraction of low angle grain boundaries (2°~15°) in the sample extruded at 420 °C is 13.61%, which is lower than that of extruded at 360 °C (19.93%). The low angle boundaries are mainly distributed in the unDRX regions, which suggests that the low angle boundaries transfer into high angle boundaries during the DRX process. The texture exerts an effect on the mechanical properties according to restricting the number of slip systems available in the Mg alloys<sup>[19]</sup>. Consequently, in order to assess the effect of texture on strength, the Schmid factors in terms of basal slip, (0001)[1120] are shown in Fig.5b and 5d. The average Schmid factor of sample extruded at 360 °C is lower than that of sample extruded at 420 °C. The average Schmid factors are

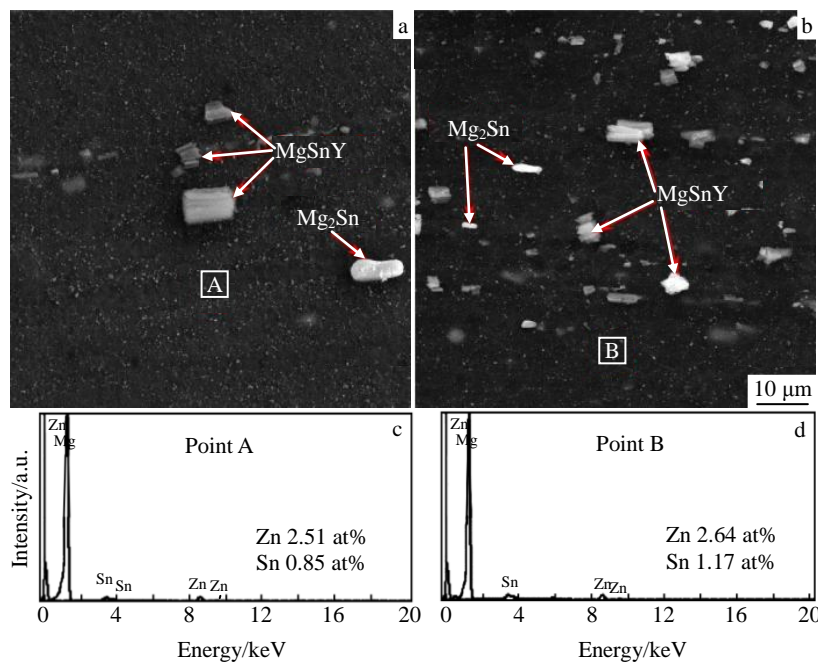


Fig.3 SEM images (a, b) and EDS spectra (c, d) of ZMT614-0.5Y alloy extruded at different temperatures: (a, c) 360 °C and (b, d) 420 °C

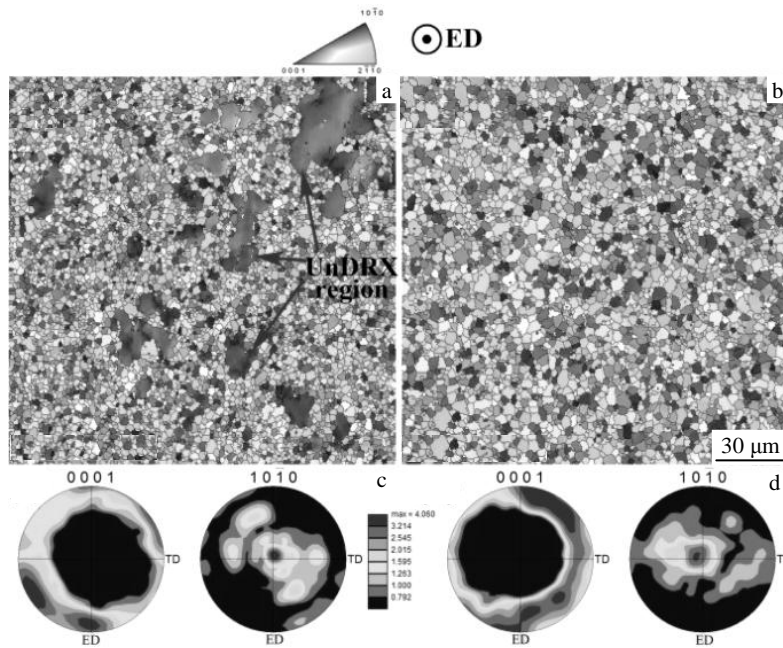


Fig.4 IPF and PFs of ZMT614-0.5Y alloy extruded at different temperatures: (a, c) 360 °C and (b, d) 420 °C

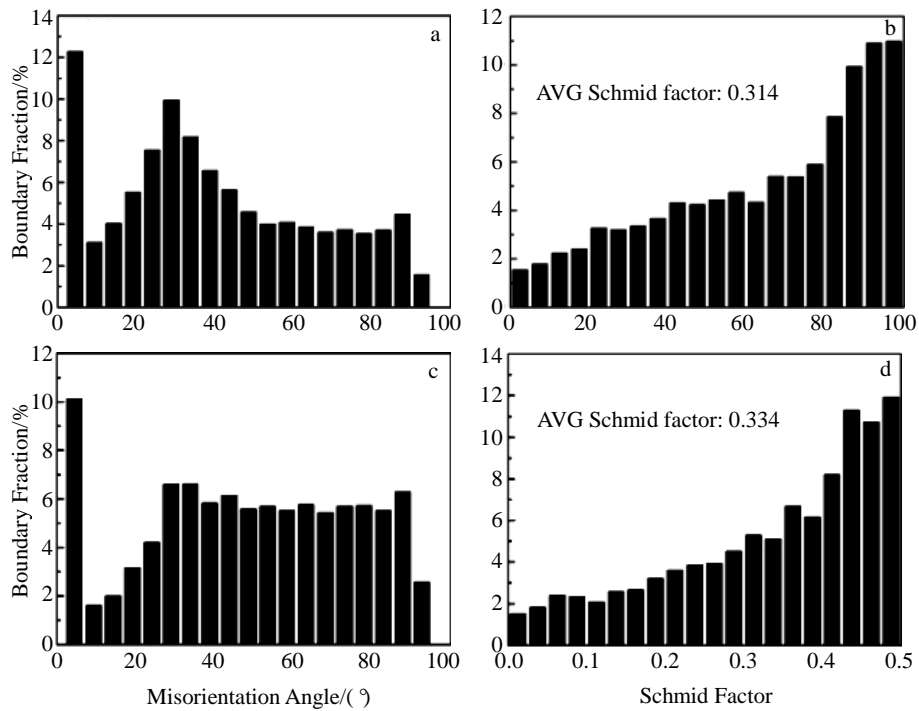


Fig.5 Misorientation angle (a, c) and Schmid factors (b, d) of ZMT614-0.5Y alloy extruded at different temperatures: (a, b) 360 °C and (c, d) 420 °C

0.314 and 0.334, respectively, revealing that the unDRX regions possess lower average Schmid factors compared with the DRX regions. Consequently, the unDRX regions do not easily yield when the tensile stress is applied parallel to the ED<sup>[18]</sup>. The tensile strength of ZMT614-0.5Y alloy decreases as the extrusion temperature increases.

## 2.2 Mechanical properties of as-extruded alloy

The mechanical properties of as-extruded samples at room temperature are shown in Fig.6. When extruded at 360 °C, the yield strength (YS), ultimate tensile strength (UTS) and elongation (EL) are 259 MPa, 350 MPa and 18.3%, respectively. The strength and the elongation decrease as the extrusion temperature increases. The YS, UTS and elongation decrease by 20 MPa, 18 MPa and 5.8%, respectively, when

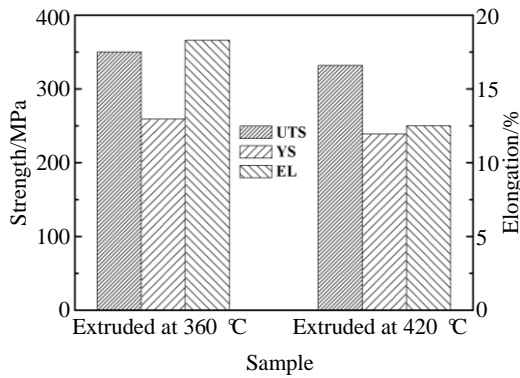


Fig.6 Tensile properties of the ZMT614-0.5Y samples extruded at 360 and 420 °C

extruded at 420 °C.

The extrusion temperature exerts a substantial effect on the mechanical properties of as-extruded samples. As the extrusion temperature increases, the grains become coarse, the Schmid factor increases, and the amount of fine Mg<sub>7</sub>Zn<sub>3</sub> particles decreases obviously. During the deformation, the dislocation motion and twins arise in grains by the applied stress. The main slips of Mg alloys are basal slip (0001)[1120], prismatic slip (1010)[1120], pyramidal slips (1011)[1120] and (1012)[1120]. However, the critical resolved shear stress (CRSS) ratios of the three slip systems are 1:38:50<sup>[20]</sup>. Thus, the basal slip is activated easily during the deformation. It is supposed that only the basal slip is activated, the YS could be described as follows:

$$\sigma_{ys} = \frac{\tau_c}{m} \quad (1)$$

where  $\sigma_{ys}$  and  $\tau_c$  are YS and CRSS, respectively,  $m$  is Schmid factor of basal slip. According to the Eq.(1), the YS is in inverse proportion to Schmid factor. The average Schmid factors of the two samples are 0.314 and 0.334, respectively. Therefore, the YS decreases as the extrusion temperature increases.

During the deformation, the dispersive second phase particles improve the YS by inhibiting the climbing and sliding of dislocations. Based on the Orowan dislocation bypass mechanism, the increment of YS ( $\Delta\sigma_{sp}$ ) is given as follows<sup>[21]</sup>:

$$\Delta\sigma_{sp} = \frac{Gb}{2\pi\lambda A} \ln \frac{d_p}{r_0} \quad (2)$$

where  $G$  is the shear modulus of the matrix,  $b$  is the magnitude of the Burgers vector of the slip dislocations,  $A$  is a constant,  $\lambda$  is the effective planar inter-obstacle spacing,  $d_p$  is the mean planar diameter of the point obstacles, and  $r_0$  is the core radius of dislocations. Nie<sup>[21]</sup> reported that the YS was proportional to the density of second phase particles. As shown in Fig.3, when the extrusion temperature increases, the density of second phase particles decreases and leads to the YS

decreasing.

For as-extruded Mg alloy, refined grains could improve its mechanical properties remarkably. The improvement of YS ( $\Delta\sigma_{rg}$ ) can be estimated by the Hall-Petch law as follows:

$$\Delta\sigma_{rg} = \sigma_{Mg} + kd^{-1/2} \quad (3)$$

where  $\sigma_{Mg} = 11$  MPa for pure Mg,  $k = 220$  MPa  $\mu\text{m}^{1/2}$  for Mg alloy<sup>[12]</sup>.  $d$  are 3.2 and 5.7  $\mu\text{m}$  for the as-extruded samples. Then  $\Delta\sigma_{rg}$  are 134 and 103 MPa, respectively. According to the calculations, the YS decreases by 31 MPa when the extrusion temperature increases to 420 °C, which is somewhat higher than the experimental one (20 MPa).

For as-extruded Mg alloys, the solid solution atoms could make the enhancement in YS ( $\Delta\sigma_{ss}$ ). To quantitatively estimate their contributions, a widely used models were employed<sup>[22]</sup>. The models supposed that the matrix was in an ideal state.

$$\Delta\sigma_{ss} = \left( \sum_i k_i^{1/n} c_i \right)^n \quad (4)$$

where  $n = 2/3$ ,  $c_i$  and  $k_i$  are the concentration of solute  $i$  and the strengthening coefficient for solute  $i$ , respectively. EDS reveals that the main solid solution elements are Sn and Zn in the as-extruded alloys, and their combinative contributions to the enhancement of YS is expressed as follows:

$$\Delta\sigma_{ss} = (k_{Zn}^{3/2} C_{Zn} + k_{Sn}^{3/2} C_{Sn})^{2/3} \quad (5)$$

where the values of  $C_{Zn}$  and  $C_{Sn}$  are shown in Fig.3.  $k_{Zn} = 905$  MPa (at%)<sup>-2/3</sup> and  $k_{Sn} = 389$  MPa (at%)<sup>-2/3</sup> for solid solution elements Zn and Sn<sup>[12]</sup>, respectively. Substituting  $k$  and  $C$  into Eq.(5), the  $\Delta\sigma_{ss}$  are 82 and 87 MPa, respectively. When the extrusion temperature increases, the strength only decreases by 5 MPa. It demonstrates that extrusion temperature has a little effect on the solid solution strengthening.

Respecting the above analysis, the enhancement YS of as-extruded ZMT614-0.5Y alloy should be expressed as follows:

$$\sigma_{ys} = \Delta\sigma_{Mg} + \Delta\sigma_{sp} + \Delta\sigma_{rg} + \Delta\sigma_{ss} \quad (6)$$

Based on the Eq.(6), the theoretical  $\sigma_{ys}$  values of the two samples are (237 +  $\Delta\sigma_{sp}$ ) and (201 +  $\Delta\sigma_{sp}$ ) MPa, respectively. Compared with the experimental YS, the  $\Delta\sigma_{sp}$  values of the two samples are estimated to be 20 and 40 MPa, respectively. They are much lower than the values of  $\Delta\sigma_{rg}$  and  $\Delta\sigma_{ss}$ . The fine grain strengthening and solid solution strengthening make the largest contribution to the enhancement of YS.

### 3 Conclusions

- 1) The phase compositions of as-cast and extruded alloys consist of  $\alpha$ -Mg, Mn, Mg<sub>7</sub>Zn<sub>3</sub>, Mg<sub>2</sub>Sn, and MgSnY phases.
- 2) As the extrusion temperature increases from 360 °C to 420 °C, dynamic recrystallization is completed and grain growth occurs. The YS, UTS and elongation decrease by 20 MPa, 18 MPa and 5.8%, respectively.
- 3) For the as-extruded samples, the strengthening mechanism could not change when the extrusion temperature increases. The

grain size strengthening, and solid solution strengthening make the largest contribution to enhancement of YS.

## References

- 1 Li J L, Chen R S, Ma Y Q et al. *Journal of Magnesium and Alloys*[J], 2013, 1(1): 64
- 2 Qi F G, Zhang D F, Lan W et al. *Rare Metal Materials and Engineering*[J], 2013, 42(1): 115 (in Chinese)
- 3 Mao P L, Yu J C, Liu Z et al. *Journal of Magnesium and Alloys*[J], 2013, 1(1): 64
- 4 Mendis C L, Oh-ishi K, Ohkubo T et al. *Materials Science and Engineering A*[J], 2012, 553: 9
- 5 Xie S Y, Peng X D, Li J C et al. *Rare Metal Materials and Engineering*[J], 2014, 43(1): 52 (in Chinese)
- 6 Zhu Q, Fang C F, Li N P et al. *Rare Metal Materials and Engineering*[J], 2013, 42(4): 771 (in Chinese)
- 7 Mendis C L, Oh-ishi K, Kawamura Y et al. *Acta Materialia*[J], 2009, 57(3): 749
- 8 Yoon D J, Lee S, Lim S J et al. *Journal of Mechanical Science and Technology*[J], 2010, 24(1): 131
- 9 Xu S W, Oh-ishi K, Kamado S et al. *Scripta Materialia*[J], 2011, 65(10): 875
- 10 Zhang L, Gong M, Peng L M. *Materials Science and Engineering A*[J], 2013, 565: 262
- 11 Gao L, Chen R S, Han E H. *Journal of Alloys and Compounds*[J], 2009, 481(1-2): 379
- 12 Shi B Q, Chen R S, Ke W. *Journal of Alloys and Compounds*[J], 2011, 509(7): 3357
- 13 Oh-ishi K, Mendis C L, Homma T et al. *Acta Materialia*[J], 2009, 57(18): 5593
- 14 Borkar H, Pekguleryuz M. *Journal of Materials Science*[J], 2013, 48(4): 1436
- 15 Sadeghi A, Pekguleryuz M. *Journal of Materials Science*[J], 2012, 47(14): 5374
- 16 Zhao H D, Qin G W, Ren Y P et al. *Journal of Alloys and Compounds*[J], 2009, 481(1-2): 140
- 17 Gorny A, Bamberger M, Katsman A. *Journal of Materials Science*[J], 2007, 42(24): 10 014
- 18 Homma T, Hirawatari S, Sunohara H et al. *Materials Science and Engineering A*[J], 2012, 539: 163
- 19 Xia X S, Zhang K, Li X G et al. *Materials & Design*[J], 2013, 44: 521
- 20 Gehrmann R, Frommert M M, Gottstein G. *Materials Science and Engineering A*[J], 2005, 395(1-2): 338
- 21 Nie J F. *Scripta Materialia*[J], 2003, 48(8): 1009
- 22 Li Z M, Fu P H, Peng L M et al. *Journal of Materials Science*[J], 2013, 48(1): 1

## 挤压温度对 Mg-6Zn-1Mn-4Sn-0.5Y 镁合金组织和性能的影响

胡光山<sup>1,2</sup>, 张丁非<sup>1,2</sup>, 唐甜<sup>1,2</sup>, 蒋璐瑶<sup>1,2</sup>, 潘复生<sup>1,2</sup>

(1. 重庆大学, 重庆 400045)

(2. 国家镁合金材料工程技术中心, 重庆 400044)

**摘要:** 通过光学显微镜 (OM), X 射线衍射 (XRD), 扫描电子显微镜 (SEM), 电子背散射衍射 (EBSD) 以及拉伸试验对 360 和 420 °C 挤压的 Mg-6Zn-1Mn-4Sn-0.5Y 变形镁合金的组织 and 性能进行了研究。结果表明, 合金铸态和时效态的相组成为  $\alpha$ -Mg, Mn, Mg<sub>7</sub>Zn<sub>3</sub>, Mg<sub>2</sub>Sn, 和 MgSnY 相。挤压温度从 360 °C 增加到 420 °C, 动态再结晶完成, 晶粒长大, 合金的屈服强度、抗拉强度以及延伸率分别由 259 MPa, 350 MPa 和 18.3% 降低至 239 MPa, 332 MPa 和 12.5%。理论计算和拉伸试验结果表明, 细晶强化和固溶强化对合金屈服强度的增加产生决定性影响。

**关键词:** Mg-6Zn-1Mn-4Sn-0.5Y 镁合金; 挤压温度; 相组成; 力学性能

作者简介: 胡光山, 男, 1986 年生, 博士, 重庆大学材料科学与工程学院, 重庆 400045, 电话: 023-65112491, E-mail: beixue10@163.com